Biogeosciences Discuss., 12, 9497–9541, 2015
www.biogeosciences-discuss.net/12/9497/2015/
doi:10.5194/bgd-12-9497-2015

Biogeosciences Discussions
Open Access

Ecosystem model-based approach for modelling the dynamics of ^{137}Cs transfer to marine plankton populations: application to the western North Pacific Ocean after the Fukushima nuclear power plant accident

M. Belharet[1,2], C. Estournel[2], and S. Charmasson[1]

[1]Institut de Radioprotection et de Sûreté nucléaire, ENV-PRP/SESURE/LERCM, 83507, CS20330, La Seyne-Sur-Mer, France
[2]Laboratoire d'aérologie (LA), UMR5560, CNRS, Université de Toulouse, UPS, 14 avenue Edouard Belin, 31400 Toulouse, France

Received: 18 May 2015 – Accepted: 03 June 2015 – Published: 26 June 2015

Correspondence to: M. Belharet (mokrane.belharet@gmail.com)

Published by Copernicus Publications on behalf of the European Geosciences Union.

Title Page
Abstract | Introduction
Conclusions | References
Tables | Figures
◀| |▶
◀ ▶
Back | Close
Full Screen / Esc
Printer-friendly Version
Interactive Discussion

Abstract

Huge amounts of radionuclides, especially ^{137}Cs, were released into the western North Pacific Ocean after the Fukushima nuclear power plant (FNPP) accident that occurred on 11 March 2011, resulting in contamination of the marine biota. In this study we developed a radioecological model to estimate ^{137}Cs concentrations in phytoplankton and zooplankton populations representing the lower levels of the pelagic trophic chain. We coupled this model to a lower trophic level ecosystem model and an ocean circulation model to take into account the site-specific environmental conditions in the area. The different radioecological parameters of the model were estimated by calibration, and a sensitivity analysis to parameter uncertainties was carried out, showing a high sensitivity of the model results, especially to the ^{137}Cs concentration in seawater, to the rates of uptake from water and to the radionuclide assimilation efficiency for zooplankton. The results of the ^{137}Cs concentrations in planktonic populations simulated in this study were then validated through comparison with the some data available in the region after the accident. The model results have shown that the maximum concentrations in plankton after the accident were about two to four orders of magnitude higher than those observed before the accident depending on the distance from FNPP. Finally, the maximum ^{137}Cs absorbed dose rate for phyto- and zooplankton populations was estimated to be about 10^{-2} µGy h^{-}1, and was, therefore, lower than the 10 µGy h^{-1} benchmark value defined in the ERICA assessment approach from which a measurable effect on the marine biota can be observed.

1 Introduction

Huge amounts of radionuclides, especially ^{137}Cs, were released into the western North Pacific Ocean after the Fukushima nuclear power plant (FNPP) accident that occurred on 11 March 2011 (UNCEAR, 2014).

BGD
12, 9497–9541, 2015

Plankton populations, which play a prominent role in the input of many pollutants into the aquatic food chain (Bettinetti and Manca, 2013), were largely affected by this contamination. Within a few months following the accident, zooplankton collected at some locations of the western North Pacific showed enhanced levels of ^{137}Cs, even for the samples collected at the farthest locations from FNPP, such as the S1 (47° N, 160° E, 1900 km from FNPP) and K1 (30° N, 145° E, 900 km from FNPP) stations where the ^{137}Cs in zooplankton observed one month after the accident were two orders of magnitude higher than before 11 March (Honda et al., 2012). Three months after the accident, Buesseler et al. (2012) reported that the ^{137}Cs concentrations in zooplankton located at 300–600 km from FNPP were two to three orders of magnitude higher than before the accident. Even 10 months after the accident, the ^{137}Cs concentrations observed in zooplankton, at 600–2100 km away from FNPP, were still about one to two orders of magnitude higher than in the pre-accident period (Kitamura et al., 2013).

Although these field data provide a general overview of the plankton contamination levels after the FNPP accident, the lack of information on the contamination's temporal and spatial evolution and the need for understanding the fate of radionuclides in the marine ecosystem, necessary for the assessment of environmental and human health consequences, require the adaptation of a modelling method (Monte et al., 2009).

The simple linear method based on the bioconcentration factor, defined as the ratio of the amount of radionuclide in the organism divided by the concentration in the water, is the most commonly used to assess the radionuclide concentration in marine biota (Buesseler, 2014). Despite its simplicity, this method is not appropriate in an accident situation since the main underlying hypothesis, i.e. an equilibrium state between the radionuclide concentration in water and biota, is not reached.

Rates of both radionuclide uptake and loss are known to be affected by species metabolism. Moreover, it has been reported that a large part of the accumulated radionuclides by heterotrophic marine biota comes from food (Kasamatsu and Ishikawa, 1997; Rowan, 2013; Thomann, 1981; Zhao et al., 2001), and that the photosynthesis process plays a prominent role in the regulation of the radionuclide concentration in

BGD
12, 9497–9541, 2015

primary producer populations (Gutknecht, 1965; Williams, 1960; Yousef et al., 1975). Therefore, the characterization of the radionuclide distribution in these components should be accompanied by ecological information such as species composition in the ecosystem, population densities, rates of primary and secondary production, food ingestion rate, etc. (IAEA, 1975). Such parameters are generally influenced by various environmental factors (light, temperature, salinity, food availability, marine hydrodynamics) that vary quickly from one site to another according to geographic location and morphological characteristics (bathymetry, distance from the shore).

Consequently, the effective consideration of all these factors implies that the modelling approach of radionuclide transfer to marine biota should be driven by an ecosystem model describing different ecological processes and transfers between organisms in the food web (Erichsen et al., 2013; Koulikov and Meili, 2003; Kryshev and Ryabov, 2000; Kumblad et al., 2006; Sandberg et al., 2007).

In this study, we developed a generic radioecological model to estimate the ^{137}Cs concentration in marine plankton populations. This model was applied to study ^{137}Cs transfer to plankton populations in the western North Pacific after the FNPP accident and to compare it with the pre-accident steady state situation. The NEMURO ecosystem model (Kishi et al., 2007) was used to simulate the planktonic population dynamics in the area and to estimate different ecological fluxes. It was coupled to the hydrodynamic SYMPHONIE model (Marsaleix et al., 2008) in order to account for the impact of hydrodynamic and hydrologic conditions on the dynamics of organic and inorganic compounds. The ^{137}Cs concentrations in seawater after the accident were obtained from dispersion numerical simulations.

2 Material and methods

The modelling method used in this study aims to estimate the activity concentration of ^{137}Cs in different plankton populations, to analyse its sensitivity to the model parameter uncertainties, and to understand the transfer mechanism and its relation with the ecological functioning of the living organisms. It is based on three different models: (1) a 3-D hydrodynamic model simulating the movement of dissolved and particulate state variables of the ecosystem model and estimating the physicochemical characteristics of seawater (temperature, salinity), (2) an ecosystem model simulating the plankton biomasses and their different metabolic rates and fluxes (e.g. primary production, excretion, grazing, mortality, etc.), and (3) a mechanistic radioecological model simulating the ^{137}Cs concentration in different plankton populations.

2.1 Hydrodynamic modelling

We used the three-dimensional SYMPHONIE ocean circulation model (Marsaleix et al., 2009a, 2009b, 2012). This model has been widely used in the Mediterranean Sea to study different marine processes related to coastal circulation (Estournel et al., 2003; Petrenko et al., 2008), sediment transport (Ulses et al., 2008), larval dispersal (Guizien et al., 2012) and plankton population dynamics (Auger et al., 2011; Herrmann et al., 2014). This model has also been used, for the first time, in the western North Pacific Ocean to study the ^{137}Cs dispersion after the FNPP accident (Estournel et al., 2012).

The numerical configuration used in this study was the same as the one reported in detail by (Estournel et al., 2012), with 30 vertical irregular levels based on the sigma coordinate system and characterized by an increase of resolution near the surface. The horizontal grid (Fig. 1) corresponds to an orthogonal curvilinear system, with variable resolution increasing linearly with the distance from FNPP (0.6 × 0.6 km near FNPP and 5 × 5 km at the open lateral boundaries off Japan).

2.2 Ecosystem modelling

To properly represent the dynamics of the plankton populations exposed to the radioactive contamination in our study area, the NEMURO biogeochemical model (Kishi et al., 2007) was applied. This model, which has been extensively used in the western North Pacific region (Aita et al., 2003; Hashioka and Yamanaka, 2007; Komatsu et al., 2007), consists of 11 state variables with two size-classes of phytoplankton: small phytoplankton (PS) representing small species such as coccolithophorids and flagellates, and large phytoplankton (PL) representing diatoms. It includes three size-classes of zooplankton: small zooplankton (ZS) such as ciliates and foraminifera, large zooplankton (ZL) (copepods), and predatory zooplankton such as krill and/or jellyfish. The other model state variables are: nitrate (NO_3), ammonium (NH_4), silicate ($Si(OH)_4$), particulate organic nitrogen (PON), biogenic silica (Opal) and dissolved organic nitrogen (DON). The model structure and the different parameter values are presented in detail in Kishi et al. (2007).

2.3 Radioecological modelling

2.3.1 Phytoplankton

The knowledge of the ^{137}Cs accumulation mechanisms in aquatic primary producers, mainly phytoplankton, is still vague. However, previous studies underlined that it is mostly transported into the cell by active absorption since it is an alkali metal analogue of potassium (Fukuda et al., 2014). Therefore, the dynamics of radionuclide concentration in phytoplankton populations is determined by a balance between radionuclide concentration in seawater, the biological half-life of clearance, and different processes affecting the population biomasses:

$$\frac{\mathrm{d}[\mathrm{Cs}]_\mathrm{p}}{\mathrm{d}t} = \mu_\mathrm{p}[\mathrm{Cs}]_\mathrm{w} - \left(m_\mathrm{p} + m_\mathrm{p}^\mathrm{G}\right)[\mathrm{Cs}]_\mathrm{p} - \frac{1}{B_\mathrm{p}}\frac{\mathrm{d}B_\mathrm{p}}{\mathrm{d}t}[\mathrm{Cs}]_\mathrm{p} - (\lambda_{\mathrm{p_B}} + \lambda_{\mathrm{p_P}})[\mathrm{Cs}]_\mathrm{p} \tag{1}$$

where $[\mathrm{Cs}]_\mathrm{p}$ is the ^{137}Cs concentration in the phytoplankton population ($\mathrm{Bq\,g^{-1}}$ wet weight), $[\mathrm{Cs}]_\mathrm{w}$ is the ^{137}Cs concentration in the seawater ($\mathrm{Bq\,L^{-1}}$), B_p is the phytoplankton biomass ($\mathrm{\mu molN\,L^{-1}}$), m_p and m_p^G are, respectively, the natural mortality rate and the rate of mortality due to the grazing ($\mathrm{d^{-1}}$), $\lambda_{\mathrm{p_B}}$ and $\lambda_{\mathrm{p_P}}$ are, respectively, the

BGD
12, 9497–9541, 2015

biological depuration rate of ^{137}Cs from phytoplankton and the ^{137}Cs physical decay rate (d^{-1}), and μ_p is the ^{137}Cs accumulation rate by the phytoplankton ($L\,g^{-1}\,d^{-1}$).

In the NEMURO ecosystem model, the phytoplankton population growth rate is given by the equation:

$$\frac{1}{B_p}\frac{dB_p}{dt} = pp - exc_p - R_p - m_p - m_p^G \tag{2}$$

where exc_p and R_p are, respectively, the phytoplankton excretion and respiration rates (d^{-1}), and pp the gross primary production rate (d^{-1}). After rearrangement we obtain from Eqs. (1) and (2):

$$\frac{d[Cs]_p}{dt} = \mu_p[Cs]_w - \left(pp - exc_p - R_p + \lambda_p\right)[Cs]_p \tag{3}$$

where $\lambda_p = \lambda_{p_P} + \lambda_{p_B}$.

2.3.2 Zooplankton

The dynamics of radionuclide concentration in consumers reflects the variation over time of the radionuclide intake from both water and food. Therefore, the differential equation describing the dynamics of ^{137}Cs concentration in the zooplankton populations can be written as:

$$\frac{d[Cs]_z}{dt} = \mu_z[Cs]_w + AE_z\sum_{j=1}^{N} IR_{j\to z}[Cs]_j - \left(m_z + m_z^G + \lambda_{z_B} + \lambda_{z_P} + \frac{1}{B_z}\frac{dB_z}{dt}\right)[Cs]_z \tag{4}$$

where $[Cs]_z$, $[Cs]_j$ and $[Cs]_w$ represent, respectively, the ^{137}Cs concentrations in zooplankton, in prey index j ($Bq\,g^{-1}$ ww) and in seawater ($Bq\,L^{-1}$), B_z is the zooplankton biomass ($\mu molN\,L^{-1}$), μ_z is the ^{137}Cs accumulation rate by zooplankton population

BGD
12, 9497–9541, 2015

(d^{-1}), AE_z is the assimilation efficiency of ^{137}Cs by zooplankton, $IR_{j\rightarrow z}$ is the ingestion rate of prey index j by the zooplankton, N represents the number of prey populations present in the area that are available for the zooplankton, λ_{z_B} and λ_{z_P} are, respectively, the biological depuration rate (d^{-1}) of the ^{137}Cs by the zooplankton and the ^{137}Cs radioactive physical decay rate (d^{-1}), and m_z and m_z^G are, respectively, the zooplankton natural and grazing mortality rates (d^{-1}).

The zooplankton population growth rate is modelled in the NEMURO model as follows:

$$\frac{1}{B_z}\frac{dB_z}{dt} = \left(\sum_{j=1}^{N} IR_{j\rightarrow z}\right) - exc_z - ege_z - m_z - m_z^G \tag{5}$$

where exc_z and ege_z are, respectively, the excretion and egestion rates (d^{-1}). After rearrangement of equations modelled in the NEMURO model we obtain:

$$exc_z + ege_z = (1-b)\sum_{j=1}^{N} IR_{j\rightarrow z} \tag{6}$$

where b is the growth efficiency of zooplankton. By inserting Eq. (5) into Eq. (4), and considering Eq. (6), we can write:

$$\frac{d[Cs]_z}{dt} = \mu_z[Cs]_w + AE_z\left(\sum_{j=1}^{N} IR_{j\rightarrow z}[Cs]_j\right) - \left(\lambda_z + b\sum_{j=1}^{N} IR_{j\rightarrow z}\right)[Cs]_z \tag{7}$$

where $\lambda_z = \lambda_{z,p} + \lambda_{z_B}$.

2.4 Model simulation

The ocean circulation model (OCM) was run from February 2010 to January 2013. The currents, vertical diffusivities and temperature fields were then used to force the

BGD
12, 9497–9541, 2015

ecosystem model and spun-up for 3 years by repeating the same forcing data for the first two years. For this study, we used the results of the two last simulated years (February 2011 to December 2012), when a quasi-steady state was reached.

To assess the effect of the accident on the planktonic populations, two different simulations were carried out: (1) the real situation with the presence of the contaminated waters due to the accident on 11 March 2011, and (2) a no-accident situation by assuming a steady state situation over the whole simulation period.

Before the accident date (11 March 2011), the seawater ^{137}Cs concentration for the western North Pacific Ocean ranged from 1 to 2 $mBq\,L^{-1}$ (Povinec et al., 2013). For the purposes of the modelling, a constant ^{137}Cs concentration in seawater of 2 $mBq\,L^{-1}$ is assumed throughout the study area. In the accident situation, we used, as of 11 March 2011, the ^{137}Cs concentrations in seawater obtained from the dispersion simulation carried out by Estournel et al. (2012).

2.5 Model calibration and sensitivity analysis

The radioecological parameters related to plankton are very scarce, and are often associated with considerable uncertainties. In this study, a temporal series of the ^{137}Cs concentration in zooplankton collected at Sendai Bay (MEXT, 2014) between June 2011 and December 2013 was used to calibrate the model and estimate the different radioecological parameters. However, there was no indication on the relative composition and geographical positions of these field data, therefore for the purpose of the modelling we used the weighted mean of the ^{137}Cs concentrations in the three zooplankton groups, and we considered that the Sendai Bay is represented by the marine area situated between 37.6–38° N and 140–142° W.

To assess the sensitivity of the calibrated parameters, we investigated a sensitivity analysis of the radioecological model using the classical one-parameter-at-a-time analysis (OAT). The choice of this quantitative method can be justified by its simplicity and by the absence of any interactive effects among parameters. In this local approach, the single parameter variation effect is estimated by increasing and decreasing each

BGD
12, 9497–9541, 2015

parameter in Eqs. (3) and (7) by 10 %, while keeping all the others fixed at their nominal values. The sensitivity S_p associated with each parameter p was computed as the percentage of change in activity generated by the parameter variation:

$$S_p\,(\%) = \frac{E\,(p) - E}{E} \cdot 100$$

where $E\,(p)$ is the prognostic variable value (here, the ^{137}Cs concentration in plankton populations) when the parameter p is set to its changed value (10 % higher or lower than its calibrated value), and E is the value of the prognostic variable in the baseline run (i.e., all parameters at their calibrated values).

2.6 Absorbed dose rate

To assess the biological effects of the ^{137}Cs ionizing radiation on the plankton populations, we calculated the absorbed dose rate from internal and external pathways using the FASSET dose assessment approach (Pröhl, 2003). This approach consists in converting the ^{137}Cs concentration in plankton populations and in seawater to the internal and external absorbed dose rates, respectively, using the so-called "Dose Conversion Coefficients", which are specific for each radionuclide-organism combination. The different dose rates are calculated as follows:

$$D = D_{\text{int}} + D_{\text{ext}}$$

$$D_{\text{int}} = \text{DCC}_{\text{Cs-pk}}\,[\text{Cs}]_{\text{pk}}$$

$$D_{\text{ext}} = \text{DCC}_{\text{Cs-w-pk}}\,[\text{Cs}]_{\text{w}}$$

where D , D_{int}, D_{ext} are, respectively, the total, the internal and the external dose rates (μGy h^{-1}), $[\text{Cs}]_{\text{pk}}$ and $[\text{Cs}]_{\text{w}}$ are, respectively, the ^{137}Cs concentration in plankton population and seawater (in Bq kg^{-1}), $\text{DCC}_{\text{Cs-pk}}$ is the dose conversion coefficient for the

BGD
12, 9497–9541, 2015

internal exposure, and $DCC_{Cs\text{-}w\text{-}pk}$ represents the dose conversion coefficient for external exposure (in $\mu Gy\,h^{-1}$ per $Bq\,kg^{-1}$).

The DCC parameter values for phytoplankton and zooplankton used in this study are obtained from the coastal aquatic ecosystem DCCs reported by Pröhl (2003). The values of these parameters are summarized in Table 3.

3 Results and discussions

3.1 Validation of the ecosystem model, and zooplankton taxonomic compositions

The seasonal variations in phytoplankton and zooplankton biomasses were presented for three different areas classified according to latitude: the subtropical region (latitude $< 35^\circ$ N), the transition region (35° N $<$ latitude $< 39^\circ$ N), and the subarctic region (latitude $> 39^\circ$ N) (Fig. 1). The ecosystem model outputs are expressed in $\mu mol\,N\,L^{-1}$, their conversion to the chlorophyll *a* unit is carried out using a C / chl ratio of 50 / 1, and a C / N ratio of 133 / 17 (Kishi et al., 2007).

The monthly medians of the spatial chlorophyll-a concentration averaged over a 50 m deep layer were used to compare model results for the period (2011–2012) with the twenty years of climatology field data (1990–2010) (Fig. 3a, c, e). In all areas, the temporal evolution of the chlorophyll standing stocks showed a seasonal cycle with higher median values in spring (April–May) and autumn (October–November). This seasonal cycle is less marked in the subtropical region than in the two other regions. The simulated chlorophyll *a* concentration medians varied from less than $0.5\,mg\,m^{-3}$ in all regions in winter to approximately 1, 1.5 and $3\,mg\,m^{-3}$ in spring in the subtropical, the transition and the subarctic regions, respectively. These values of the chlorophyll *a* concentrations are in general consistent with the field data, and show the same seasonal variability.

BGD
12, 9497–9541, 2015

The total zooplankton biomass and its taxonomic composition are presented in Fig. 3 (b, d, f) for the three regional areas described above. These modelled zooplankton biomasses showed an annual seasonality in the three regions, with minimum values in winter and peaks in spring and autumn. The zooplankton biomasses showed latitudinal variations with greater biomass in the subarctic region (from 200 mg m^{-3} wet weight in winter to about 700 mg m^{-3} wet weight in late spring), followed by the transition region (from 150 to about 500 mg m^{-3} ww) and the subtropical region (from 100 to about 300 mg m^{-3} ww).

In the subtropical region, the taxonomic composition of zooplankton biomass was dominated by large zooplankton with about 40 %, followed by small and predatory zooplankton each accounting for 30 % of the total biomass.

In the transition region, the seasonal cycle of zooplankton composition was more pronounced. In winter, the zooplankton was represented by 40 % of large zooplankton, and 30 % of small and predatory zooplanktons. In spring, the zooplankton biomass was dominated by large zooplankton (60 % ZL and 20 % for both ZS and ZP). From late spring until early autumn, the zooplankton composition changed progressively with a decrease of the ZL proportion, to be composed of 40 % ZP and 30 % of ZS and ZL in early autumn.

In the subarctic region, the proportions of small zooplankton, large zooplankton and predatory zooplankton were, respectively, 25, 35 and 40 % in winter, 10, 70 and 20 % in spring, and 20, 35 and 45 % in late summer and early autumn.

Modelled seawater temperatures showed a good agreement with the field observations (Fig. 2). The seawater temperature is an important parameter regulating the different metabolic processes, and is therefore involved in all ecological processes affecting the ^{137}Cs transfer to the biological compartments.

3.2 Model calibration

The result of the calibration is shown in Fig. 4, and the final estimated radioecological parameters are summarized in Table 1. The phytoplankton elimination rates estimated

BGD
12, 9497–9541, 2015

from this calibration (0.5 d^{-1}) were very similar to that calculated using the allometric relationship reported by Vives i Batlle et al. (2007) (0.58 d^{-1}). For the zooplankton, the obtained values ranged from 0.03 to 0.11 d^{-1}, and are also in good agreement with the literature values Thoman (1981): 0.03 d^{-1}; Vives i Batlle et al. (2007): 0.056 d^{-1}).

The ^{137}Cs assimilation efficiency by zooplankton calibrated in this study was 0.75. This value is similar to that used by Brown et al. (2006), and is slightly higher than the 0.63 observed by Mathews and Fisher (2008) for the crustacean zooplankton *Artemia salina*.

The rates of ^{137}Cs direct accumulation from water by zooplankton found in this study were about 5×10^{-4} L g^{-1} for small and large zooplankton, and about 0.001 L g^{-1} d^{-1} for predatory zooplankton. The accumulation rate corresponding to phytoplankton was 0.015 for both groups.

3.3 Sensitivity analysis

The sensitivity of the estimated ^{137}Cs activity concentrations in different plankton groups to uncertainty in the parameters of Eqs. (3) and (7) calibrated to field data at Sendai Bay was tested using the OAT method, and the results are shown in Fig. 5.

For all plankton groups, the ^{137}Cs activity estimates showed a great sensitivity to the ^{137}Cs concentration in seawater, with an activity change of 10 % for a 10% change in the seawater ^{137}Cs concentration. The ^{137}Cs activity in seawater used in this study was obtained from the numerical simulations of the ^{137}Cs dispersion using the SYMPHONIE circulation model. One can imagine that all potential biases associated with this simulation would generate the same ranges of error in the results concerning the ^{137}Cs concentration in plankton. It is, therefore, clearly important to take into consideration all these errors when interpreting the results of the radioecological model.

The ^{137}Cs activity estimates in the phytoplankton groups are very sensitive to the uptake rate from water (10 % change for a 10 % change in the parameter), and are moderately sensitive to the elimination and primary production rates (5–7 % change in

BGD
12, 9497–9541, 2015

the opposite sense), whereas the sensitivity to the daily respiration rate did not exceed 1 %. The primary production rate is, therefore, the most important ecological parameter in the estimation of ^{137}Cs concentrations in phytoplankton. It allows dilution of the ^{137}Cs concentrations in phytoplankton by promoting the growth of its populations.

For all zooplankton groups, the activity estimates were most sensitive to the change in the ^{137}Cs assimilation efficiency (AE), with an activity change of about 9 % for both small and large zooplankton. For predatory zooplankton, the activity change was slightly above 10 %, which can be explained by the direct effect of the AE parameter on ZP and the indirect effect due to the change in ZS and ZL that are preyed on by ZP.

The sensitivity to the population growth efficiency (b) was also significant with about 7 % of change. This ecological parameter, which affects the zooplankton population growth and consequently plays a role in the dilution of their ^{137}Cs concentrations, is associated with substantial uncertainty. Sushchenya (1970) reported values ranging from 4.8 to 48.9 %. The value used in this study was 30 % (Kishi et al., 2007). One can expect, therefore, an overestimation of up to 45 % or an underestimation of up to 60 % in the estimates of zooplankton ^{137}Cs concentrations.

The sensitivity to the direct uptake rate of ^{137}Cs from water by zooplankton (μ_z) was relatively low (< 4 % for the three groups of zooplankton). This can be related to the lower proportion of contamination coming from water compared to that coming from food. The variation in the depuration rate induced a relatively moderate change of 5 %.

The sensitivity to the food ingestion rate was also very low, with a proportion of change not exceeding 2 % for small zooplankton and 1 % for both large and predatory zooplankton. This is due to the dual role played by the food ingestion, which contributes both to the ^{137}Cs incorporation into consumers and to its dilution by promoting the growth of consumers (Eq. 7).

The sensitivity of the ^{137}Cs activity estimates in the three groups of zooplankton to parameters related to their different preys is also not negligible. The proportions of change varied from 1 to 9 % depending on the zooplankton group and the parameter in question. For example, the sensitivity of the ^{137}Cs concentration in ZS to the PS

BGD
12, 9497–9541, 2015

accumulation rate (μ_{ps}), the elimination rate (λ_{ps}), and the primary production rate (pp) were 9, 5 and 7 %, respectively.

This sensitivity analysis showed that the parameters related to the two groups of phytoplankton are very important for the estimation of the ^{137}Cs concentration in all plankton groups. Therefore, these parameters are key determinants of the radionuclide concentration in all marine animals of the pelagic food chain (Mathews and Fisher, 2008). Consequently, the experimental determination of these parameters, often neglected due to the difficulties characterizing the measurement of radionuclides in phytoplankton, is of the greatest importance.

3.4 Radioecological model validation and spatio-temporal evolution of contaminated plankton after the FNPP accident

The simulation results corresponding to the spatial distribution of mixed zooplankton contaminated by ^{137}Cs are shown in Fig. 6 at different times from 20 March 2011 (a few days after the accident) to 01 June 2012. The mix is calculated as the weighted average of the three zooplankton groups. In the model, the ^{137}Cs concentrations in the plankton groups were calculated in Bq g^{-1}wet weight and the conversion to the dry weight unit was carried out using a dry to wet ratio of 0.2 (Buesseler et al., 2012). These results were compared with the few available field data reported by Buesseler et al. (2012) for the period of 05–18 June 2011 and by Kitamura et al. (2013) for the period of 01–05 February 2012.

Taking into consideration the high uncertainties characterizing most of the parameters and the ^{137}Cs concentration in seawater used in this model (Sect. 3.3), one can conclude that the results of this study were in general satisfactory since the differences between simulated and observed data were overall not very significant, except for some sites where the results differed substantially from reported data, as was the case around (36° N, 144° W) where the observed value was 56.4 Bq kg^{-1} dw (Buesseler et al., 2012), whereas the simulated value was below 1 Bq kg^{-1} dw. A large part of this difference could be due to a spatial shift of the contaminated plume in the model.

BGD
12, 9497–9541, 2015

In the days following the FNPP accident, the contaminated zooplankton was essentially located in the vicinity of the power plant, with concentrations generally exceeding 100 Bq kg^{-1} dw (Fig. 6a). ^{137}Cs concentrations of about 05–10 Bq kg^{-1} dw were also estimated in zooplankton located in the open sea off Fukushima, mainly due to water contamination by atmospheric deposition.

Three months after the accident (Fig. 6b), the ^{137}Cs concentrations in the simulated zooplankton exceeded 100 Bq kg^{-1} dw at all sites situated at less than 100 km from FNPP, especially near the power plant where the concentrations reached about 1000 Bq kg^{-1} dw. Due to the dispersion of the contaminated waters, the contamination reached the zooplankton located at several distant sites (over 600 km from FNPP), leading to ^{137}Cs concentrations in zooplankton between 5–20 Bq kg^{-1} dw.

Simulated ^{137}Cs concentrations in the zooplankton remained relatively high in some locations 10 months after the accident (Fig. 6c), especially around the power plant where they ranged from about 5 to 8 Bq kg^{-1} dw.

More than one year after the accident (Fig. 6d), the simulation results showed that the ^{137}Cs activity concentrations in the zooplankton were below 1 Bq kg^{-1} dw at all study areas except around FNPP where the concentrations remained slightly above 1 Bq kg^{-1} dw.

3.5 Amplification of the ^{137}Cs concentration in plankton populations following the FNPP accident

To assess the contamination level of plankton populations in 2011, we calculated a ratio of the ^{137}Cs concentration in phytoplankton (the weighted average of PS and PL) and zooplankton (the weighted average of ZS, ZL and ZP) in the real situation to the ^{137}Cs concentration in these populations without any release linked to the FNPP accident (the no-accident situation). The results of these ratios are shown in Fig. 7.

The ratios for phytoplankton and zooplankton were very similar spatially and temporally. After the accident, the ratio increased rapidly to reach a maximum one month later. The intensity of these peaks decreased with the distance from FNPP (about 10^4

at 0–30 km from FNPP to slightly lower than 10^2 at 400–500 km from FNPP). After reaching the peak, the ratios progressively decreased over time but remained relatively high at the end of 2011 especially in the sectors situated at less than 50 km from FNPP where the ratio was still higher than 10.

The rapid decrease of ^{137}Cs in planktonic populations one year after the accident in the major parts of the study area can be explained by the different processes related either to the population ecological functioning (cells growth and death, biological elimination) or to their surrounding environment conditions especially by the horizontal and vertical mixing due to the ocean hydrodynamics. FNPP is located in an area where the east-flowing Kuroshio current and the southwest-flowing Oyashio current mix, generating complicated nearshore currents and mesoscale eddies (Buesseler, 2014), thereby favouring dispersion, regeneration, and thus dilution, of the contaminated planktonic populations in the area.

Referring to the biogeochemical cycle in the pelagic environment, part of the contaminated populations would be transferred to the pelagic higher trophic levels (planktivorous fishes, squids, etc.) by predation leading to transfer of this contamination along various trophic chains. The other part will generate, after dying, large aggregated particles, known collectively as marine snow, which rapidly reach the deep sea (Asper et al., 1992) and thus contribute to the contamination of sediment and benthic organisms, especially in the coastal area. This phenomenon was observed in the Mediterranean Sea a few days after the Chernobyl accident, generating a rapid transport of some radionuclides from surface waters to a depth of 200 m (Fowler et al., 1987). This process can be expected in the Japanese coastal area characterized by very high levels of contamination especially around FNPP.

3.6 Concentration ratio

The concentration ratio ($L\,kg^{-1}$) is defined as the ratio of radionuclide in the organism ($Bq\,kg^{-1}$ wet weight) divided by its concentration in the water ($Bq\,L^{-1}$). The dynamics

BGD
12, 9497–9541, 2015

of the calculated concentration ratios for small phytoplankton, small zooplankton and predatory zooplankton populations throughout the study area and for populations located within a radius of 30 km from FNPP over the year 2011 are shown in Fig. 8. These concentration ratios are estimated for two different situations described above (see Sect. 2.4).

The spatial median of the concentration ratios, as well as the 10–90 quantiles interval, in the no-accident situation (i.e. the steady state situation) was between 20 and 30 L kg^{-1} wet weight for small phytoplankton and between 10 in winter to slightly more than 30 L kg^{-1} during the rest of the year for small zooplankton. In the case of predatory zooplankton, the concentration ratio was a little higher, ranging from 10 to about 40 L kg^{-1} wet weight. These values are in good agreement with the reported data on plankton concentration ratios in marine ecosystems, which generally range from 11 to 50 L kg^{-1} wet weight in steady state conditions (Howard et al., 2013; IAEA, 2004) .In the sector situated at less than 30 km from FNPP (right column of Fig. 8), the concentration ratio was almost constant and seasonal variability was also very less pronounced, with about 25 L kg^{-1} for PS and 30–40 for ZS and ZP. This constancy in the estimated concentration ratios for the populations located at less than 30 km compared to those estimated for the whole study area, where a substantial decrease in the concentration ratio was observed during winter, can be related to the clear differences in food ingestion rates observed in this period between the two locations (Fig. 9). In winter, the zooplankton ingestion rates estimated for the populations located at less than 30 km were higher than those estimated for the whole study area, due essentially to the spatial heterogeneity characterizing the whole study area in terms of food availability, with the presence of some "poor" regions such as the subtropical zone where the planktonic biomasses were generally very low (see Sect. 3.1).

At the time of the releases and immediately after the accident, the concentration ratio decreased rapidly for all plankton groups signifying the collapse of the steady state situation. This is mainly due to the sudden arrival of highly contaminated waters in these areas where the living plankton populations were not yet contaminated. This decreasing phase in concentration ratio was directly followed by an increasing phase reflecting the progressive accumulation of ^{137}Cs by plankton organisms until reaching equilibrium. This phase was less marked for small phytoplankton compared to the groups of zooplankton, due to the fact that phytoplankton accumulates ^{137}Cs only from water whereas in the case of zooplankton an important part of the contamination arises from food, a process requiring some time. For the populations located at less than 30 km from FNPP the dramatic decrease in the concentration ratio in March was even more intense and longer. The time needed for these populations to regain the equilibrium was about 5–10 days for PS, 30 days for ZS and about 50 days for ZP.

3.7 Relative uptake of ^{137}Cs from diet by zooplankton

The dynamics of the ^{137}Cs fraction accumulated from diet by zooplankton estimated for both the accident and no-accident situations and in the two spatial scales are presented in Fig. 11. This fraction remained stable in the case of zooplankton living at less than 30 km from FNPP and represented more than 80 % of the total ^{137}Cs accumulated by these populations. The accident effect was only briefly apparent with a slight decrease of this value.

Conversely, the proportion estimated for zooplankton populations living in the whole area revealed a decline in winter, especially in the case of ZS for which this proportion decreased to 30 %. Because of the non-decrease in the ^{137}Cs concentration in PS during this period (Fig. 10), the decrease in the relative uptake by ZS from diet could be related to the decrease in the food ingestion rate (Fig. 9). No apparent effect of the accident on the ^{137}Cs fraction accumulated from diet was observed at this large spatial scale.

3.8 Trophic transfer factor

The trophic transfer factor (TTF), defined as the ratio of radionuclide concentration in the predator to its concentration in prey, was calculated for each zooplankton group.

BGD
12, 9497–9541, 2015

The small zooplankton has only one prey (small phytoplankton), therefore the TTF was calculated directly by dividing the ^{137}Cs concentration in the ZS by its concentration in the PS. In the case of large and predatory zooplanktons that have more than one prey (3 for each one), we considered the weighted average of the ^{137}Cs concentration in each prey.

Boxplots of predicted TTFs over 2011 for the three zooplankton groups in the accident and steady state situations are shown in Fig. 12 for the two spatial scales described above.

The predicted TTF medians in the steady state situation for ZS, ZL and ZP were, respectively, about 1.5, 1.7 and 1.2 in the sector 0–30 km from FNPP, and about 1.2, 1.45 and 1.1 in the whole study area. The TTF values calculated for the whole study area were slightly lower than those of the 0–30 km sector, reflecting the variability in ingestion rate and diet composition between the two spatial scales (Fig. 9). The lower values of ZP TTFs compared to the two other zooplankton groups may also be due to differences in their respective ingestion rate values. The correlation coefficient r between the modelled TTF related to each zooplankton group in the steady state conditions and their corresponding ingestion rates showed a good correlation for the three groups of zooplankton and in both considered spatial scales (Table 2).

The predicted TTFs in the accident situation were similar to those predicted in the steady state situation when considering the whole study area. This is due to the fact that, in the farthest sites from FNPP, where the contamination was not very high, the return to equilibrium occurred more rapidly, leading to TTFs similar to those observed before the accident although the concentrations in the predator and its preys were higher than during the pre-accident period. In the sector 0–30 km from FNPP, the predicted TTFs in the accident situation were lower than those predicted in the steady state situation. This is due to the persistence of the non-equilibrium state and the high ^{137}Cs concentrations in seawater in this area, and to the fact that zooplankton accumulates ^{137}Cs mainly from food leading to a delay in its contamination compared to its preys.

BGD
12, 9497–9541, 2015

In turn, the correlation coefficients between predicted TTFs and ingestion rates in the accident situation showed a very slight decrease when considering the whole study area, and a considerable decrease when considering only the sector 0–30 km from FNPP. This means that the instability and the non-steady state conditions characterizing the post-accident period had significant effects on this correlation.

Previous works suggested that radiocesium is the only trace element apart from Hg that may be potentially biomagnified along the food chain (Harmelin-Vivien et al., 2012; Zhao et al., 2001). In our study, the modelled TTFs were generally higher than the unity for all zooplankton groups, showing evidence of biomagnification potential at this trophic level. Mathews and Fisher (2008) reached the same general conclusion for the crustacean zooplankton *Artemia salina* feeding on phytoplankton, and reported that TTFs are directly related to the food ingestion rates, and that a consistent capacity for biomagnification exists when the food ingestion rate is high.

3.9 Absorbed dose

The estimation of the absorbed dose rate (μG h^{-1}) is an essential step enabling media/biota activity concentrations to be interpreted in terms of potential effect (Beresford et al., 2007).

The calculated dose rates received by phytoplankton and zooplankton populations located at less than 30 km from FNPP over 2011 are shown in Fig. 13. The external dose rate was about 7 times higher than the internal dose rate for phytoplankton, and about 5 times higher than the internal dose rate in the case of zooplankton, resulting in similarity between the total and the external dose rates. The total dose rates for phyto- and zooplankton were also very similar, whereas the internal dose was higher for zooplankton than for phytoplankton.

For both phyto- and zooplankton, in the steady state conditions before the accident, the dose rates were about 10^{-6} μGy h^{-1}. The maximum value was reached one month after the accident with about 0.05 μGy h^{-1}. From this date, the dose rates decreased progressively to reach about 5×10^{-5} μGy h^{-1} at the end of 2011. The calculated in-

BGD
12, 9497–9541, 2015

ternal dose rates for zooplankton in June 2011 were about 10^{-4} µGy h^{-1}, and were, therefore, about 5 times greater than those reported by Fisher et al. (2013) for copepods and euphausiids collected 30–600 km off Japan. This difference is mainly due to the fact that in this study the dose rates were calculated for the populations located at 0–30 km from FNPP, where the activity level of ^{137}Cs was higher.

The maximum dose rates calculated here were very low relative to the benchmark value corresponding to 10 µGy h^{-1} as suggested by the ERICA approach (Beresford et al., 2007), signifying that the ^{137}Cs levels were too low to cause a measurable effect on these plankton populations. However, this conclusion concerns only ^{137}Cs, we ignore whether the ionizing radiation doses due to the other radionuclides released in high quantities following the FNPP accident, such as short-lived nuclides ^{132}Te, ^{131}I and ^{134}Cs, can generate any effect on these populations.

4 Conclusions

We presented a modelling approach based on an ecosystem model to estimate the ^{137}Cs activity in marine plankton populations following the Fukushima nuclear power plant (FNPP) accident, and to understand the effect of this accident on the different processes related to the radiocesium transfer in the planktonic trophic levels. This kind of model enables calculation of the non-equilibrium dynamic processes of radionuclide transfer for the biological compartments taking into account the dynamics of the biomass and the spatio-temporal variability in the ecological parameters and environmental conditions (Sazykina, 2000).

The radioecological parameters were estimated by calibration, and the model was validated with observed ^{137}Cs data in zooplankton two months and ten months after the accident. This study showed that the maximum values of the ^{137}Cs concentrations in phytoplankton and zooplankton populations were mainly reached one month after the accident and were about two to four orders of magnitude higher than those observed before the accident depending on the distance from FNPP. This study also highlighted the presence of biomagnification potential at this trophic level, since the calculated trophic transfer factors were slightly higher than unity. This brings us to the question of the potential contamination degree of planktivorous fishes and other high trophic level organisms, and of the potential risks for the marine ecosystem and human populations.

Although the contamination degrees characterizing the seawater and the plankton populations following the FNPP accident were high, the maximum ^{137}Cs dose rates calculated for both phyto- and zooplankton were about 5×10^{-2} µGy h^{-1}, they remained lower than the benchmark value considered in this study, which corresponds to the incremental screening dose rate of 10 µGy h^{-1} defined in the ERICA assessment approach (Beresford et al., 2007). However, it is important to note that the dose rate calculated in this study concerns only ^{137}Cs, and that we ignore, at this stage, whether the ionizing radiation doses due to the other radionuclides released in high quantities following the FNPP accident can generate any effect on these populations, even though all previous studies have shown that the radioactivity levels in marine biota have generally been below the levels necessary to cause a measurable effect on populations (e.g. Vives i Batlle, 2015).

Acknowledgements. We warmly thank Caroline Ulses, Thomas Duhaut, Cyril Nguyen and Patrick Marsaleix of the Laboratoire d'Aérologie (CNRS and Toulouse university) for their continuous assistance. This work is carried out in the fram of the AMORAD project (French state financial support managed by the National Agency for Research allocated in the "Investments for the Future" framework programme under reference ANR-11-RSNR-0002). This work is also part of the EC 7th Framework project COMET (Coordination and iMplementation of a pan-Europe instrumenT for radioecology).

References

Aita, M. N., Yamanaka, Y., and Kishi, M. J.: Effects of ontogenetic vertical migration of zooplankton on annual primary production – using NEMURO embedded in a general circulation model, Fish. Oceanogr., 12, 284–290, doi:10.1046/j.1365-2419.2003.00261.x, 2003.

Asper, V. L., Deuser, W. G., Knauer, G. A., and Lohrenz, S. E.: Rapid coupling of sinking particle fluxes between surface and deep ocean waters, Nature, 357, 670–672, doi:10.1038/357670a0, 1992.

Auger, P. A., Diaz, F., Ulses, C., Estournel, C., Neveux, J., Joux, F., Pujo-Pay, M., and Naudin, J. J.: Functioning of the planktonic ecosystem on the Gulf of Lions shelf (NW Mediterranean) during spring and its impact on the carbon deposition: a field data and 3-D modelling combined approach, Biogeosciences, 8, 3231–3261, doi:10.5194/bg-8-3231-2011, 2011.

Beresford, N., Brown, J., Copplestone, D., Garnier-Laplace, J., Howard, B., Larsson, C.-M., Oughton, D., Prohl, G., and Zinger, I.: D-ERICA: An integrated approach to the assessment and management of environmental risk from ionising radiation, Description of purpose, methodology and application, A deliverable of the ERICA project FI6R-CT-2004-508847, available at: https://wiki.ceh.ac.uk/download/attachments/115017395/D-Erica.pdf?version=1&modificationDate=1263814127000&api=v2 (last access: 24 June 2015), 2007.

Bettinetti, R. and Manca, M.: Understanding the role of zooplankton in transfer of pollutants through trophic food webs, in: Zooplankton: Species Diversity, Distribution and Seasonal Dynamics, edited by: Kehayias, G., chapter 1, Nova Science Publishers Inc., Hauppauge, NY , 2013.

Brown, J., Dowdall, M., Gwynn, J. P., Børretzen, P., Selnæs, Ø. G., Kovacs, K. M., and Lydersen, C.: Probabilistic biokinetic modelling of radiocaesium uptake in Arctic seal species: verification of modelled data with empirical observations, J. Environ. Radioactiv., 88, 289–305, doi:10.1016/j.jenvrad.2006.02.008, 2006.

Buesseler, K. O.: Fukushima and Ocean Radioactivity, Oceanography, 27, 92–105, 2014.

Buesseler, K. O., Jayne, S. R., Fisher, N. S., Rypina, I. I., Baumann, H., Baumann, Z., Breier, C. F., Douglass, E. M., George, J., Macdonald, A. M., Miyamoto, H., Nishikawa, J., Pike, S. M., and Yoshida, S.: Fukushima-derived radionuclides in the ocean and biota off Japan, P. Natl. Acad. Sci. USA, 109, 5984–5988, doi:10.1073/pnas.1120794109, 2012.

Erichsen, A. C., Konovalenko, L., Møhlenberg, F., Closter, R. M., Bradshaw, C., Aquilonius, K., and Kautsky, U.: Radionuclide transport and uptake in coastal aquatic ecosystems: a comparison of a 3D dynamic model and a compartment model, Ambio, 42, 464–475, doi:10.1007/s13280-013-0398-2, 2013.

Estournel, C., de Madron, X. D., Marsaleix, P., Auclair, F., Julliand, C., and Vehil, R.: Observation and modeling of the winter coastal oceanic circulation in the Gulf of Lion under wind

conditions influenced by the continental orography (FETCH experiment), J. Geophys. Res.-Oceans, 108, 8059, doi:10.1029/2001JC000825, 2003.
Estournel, C., Bosc, E., Bocquet, M., Ulses, C., Marsaleix, P., Winiarek, V., Osvath, I., Nguyen, C., Duhaut, T., Lyard, F., Michaud, H., and Auclair, F.: Assessment of the amount of cesium-137 released into the Pacific Ocean after the Fukushima accident and analysis of its dispersion in Japanese coastal waters, J. Geophys. Res.-Oceans, 117, C11014, doi:10.1029/2012JC007933, 2012.
Fisher, N. S., Beaugelin-Seiller, K., Hinton, T. G., Baumann, Z., Madigan, D. J., and Garnier-Laplace, J.: Evaluation of radiation doses and associated risk from the Fukushima nuclear accident to marine biota and human consumers of seafood, P. Natl. Acad. Sci. USA, 110, 10670–10675, doi:10.1073/pnas.1221834110, 2013.
Fowler, S., Buatmenard, P., Yokoyama, Y., Ballestra, S., Holm, E., and Nguyen, H.: Rapid Removal of Chernobyl Fallout from Mediterranean Surface Waters by Biological-Activity, Nature, 329, 56–58, doi:10.1038/329056a0, 1987.
Fukuda, S., Iwamoto, K., Atsumi, M., Yokoyama, A., Nakayama, T., Ishida, K., Inouye, I., and Shiraiwa, Y.: Global searches for microalgae and aquatic plants that can eliminate radioactive cesium, iodine and strontium from the radio-polluted aquatic environment: a bioremediation strategy, J. Plant Res., 127, 79–89, doi:10.1007/s10265-013-0596-9, 2014.
Guizien, K., Belharet, M., Marsaleix, P., and Guarinia, J. M.: Using larval dispersal simulations for marine protected area design: Application to the Gulf of Lions (northwest Mediterranean), Limnol. Oceanogr., 57, 1099–1112, doi:10.4319/lo.2012.57.4.1099, 2012.
Gutknecht, J.: Uptake and Retention of Cesium 137 and Zinc 65 by Seaweeds1, Limnol. Oceanogr., 10, 58–66, doi:10.4319/lo.1965.10.1.0058, 1965.
Harmelin-Vivien, M., Bodiguel, X., Charmasson, S., Loizeau, V., Mellon-Duval, C., Tronczyński, J., and Cossa, D.: Differential biomagnification of PCB, PBDE, Hg and Radiocesium in the food web of the European hake from the NW Mediterranean, Mar. Pollut. Bull., 64, 974–983, doi:10.1016/j.marpolbul.2012.02.014, 2012.
Hashioka, T. and Yamanaka, Y.: Seasonal and regional variations of phytoplankton groups by top-down and bottom-up controls obtained by a 3D ecosystem model, Ecol. Model., 202, 68–80, doi:10.1016/j.ecolmodel.2006.05.038, 2007.
Herrmann, M., Estournel, C., Adloff, F., and Diaz, F.: Impact of climate change on the north-western Mediterranean Sea pelagic planktonic ecosystem and associated carbon cycle, J. Geophys. Res.-Oceans, 119, 5815–5836, doi:10.1002/2014JC010016, 2014.

BGD
12, 9497–9541, 2015

Modelling of Fukushima-derived ^{137}Cs transfer to plankton populations

M. Belharet et al.

Honda, M. C., Aono, T., Aoyama, M., Hamajima, Y., Kawakami, H., Kitamura, M., Masumoto, Y., Miyazawa, Y., Takigawa, M., and Saino, T.: Dispersion of artificial caesium-134 and-137 in the western North Pacific one month after the Fukushima accident, Geochem. J., 46, E1–E9, 2012.

Howard, B. J., Beresford, N. A., Copplestone, D., Telleria, D., Proehl, G., Fesenko, S., Jeffree, R. A., Yankovich, T. L., Brown, J. E., Higley, K., Johansen, M. P., Mulye, H., Vandenhove, H., Gashchak, S., Wood, M. D., Takata, H., Andersson, P., Dale, P., Ryan, J., Bollhoefer, A., Doering, C., Barnett, C. L., and Wells, C.: The IAEA handbook on radionuclide transfer to wildlife, J. Environ. Radioactiv., 121, 55–74, doi:10.1016/j.jenvrad.2012.01.027, 2013.

IAEA: Impacts of Nuclear Releases Into the Aquatic Environment: Proceedings of an International Symposium, Otaniemi, 30 June to 4 July 1975, International Atomic Energy Agency, Vienna, 1975.

IAEA: Sediment distribution coefficients and concentration factors for biota in the marine environment, Technical report series no. 422, International Atomic Energy Agency, Vienna, available at: http://www-pub.iaea.org/MTCD/publications/PDF/TRS422_web.pdf (last access: 24 June 2015), 2004.

Kasamatsu, F. and Ishikawa, Y.: Natural variation of radionuclide Cs-137 concentration in marine organisms with special reference to the effect of food habits and trophic level, Mar. Ecol.-Prog. Ser., 160, 109–120, doi:10.3354/meps160109, 1997.

Kishi, M. J., Kashiwai, M., Ware, D. M., Megrey, B. A., Eslinger, D. L., Werner, F. E., Noguchi-Aita, M., Azumaya, T., Fujii, M., Hashimoto, S., Huang, D., Iizumi, H., Ishida, Y., Kang, S., Kantakov, G. A., Kim, H., Komatsu, K., Navrotsky, V. V., Smith, S. L., Tadokoro, K., Tsuda, A., Yamamura, O., Yamanaka, Y., Yokouchi, K., Yoshie, N., Zhang, J., Zuenko, Y. I., and Zvalinsky, V. I.: NEMURO – a lower trophic level model for the North Pacific marine ecosystem, Ecol. Model., 202, 12–25, doi:10.1016/j.ecolmodel.2006.08.021, 2007.

Kitamura, M., Kumamoto, Y., Kawakami, H., Cruz, E. C., and Fujikura, K.: Horizontal distribution of Fukushima-derived radiocesium in zooplankton in the northwestern Pacific Ocean, Biogeosciences, 10, 5729–5738, doi:10.5194/bg-10-5729-2013, 2013.

Komatsu, K., Matsukawa, Y., Nakata, K., Ichikawa, T., and Sasaki, K.: Effects of advective processes on planktonic distributions in the Kuroshio region using a 3-D lower trophic model and a data assimilative OGCM, Ecol. Model., 202, 105–119, doi:10.1016/j.ecolmodel.2006.08.023, 2007.

Koulikov, A. O. and Meili, M.: Modelling the dynamics of fish contamination by Chernobyl radiocaesium: an analytical solution based on potassium mass balance, J. Environ. Radioactiv., 66, 309–326, doi:10.1016/S0265-931X(02)00134-0, 2003.

Kryshev, A. I. and Ryabov, I. N.: A dynamic model of Cs-137 accumulation by fish of different age classes, J. Environ. Radioactiv., 50, 221–233, doi:10.1016/S0265-931X(99)00118-6, 2000.

Kumblad, L., Kautsky, U., and Naeslund, B.: Transport and fate of radionuclides in aquatic environments – the use of ecosystem modelling for exposure assessments of nuclear facilities, J. Environ. Radioactiv., 87, 107–129, doi:10.1016/j.jenvrad.2005.11.001, 2006.

Marsaleix, P., Auclair, F., Floor, J. W., Herrmann, M. J., Estournel, C., Pairaud, I., and Ulses, C.: Energy conservation issues in sigma-coordinate free-surface ocean models, Ocean Model., 20, 61–89, doi:10.1016/j.ocemod.2007.07.005, 2008.

Marsaleix, P., Auclair, F., and Estournel, C.: Low-order pressure gradient schemes in sigma coordinate models: The seamount test revisited, Ocean Model., 30, 169–177, doi:10.1016/j.ocemod.2009.06.011, 2009a.

Marsaleix, P., Ulses, C., Pairaud, I., Herrmann, M. J., Floor, J. W., Estournel, C., and Auclair, F.: Open boundary conditions for internal gravity wave modelling using polarization relations, Ocean Model., 29, 27–42, doi:10.1016/j.ocemod.2009.02.010, 2009b.

Marsaleix, P., Auclair, F., Duhaut, T., Estournel, C., Nguyen, C., and Ulses, C.: Alternatives to the Robert-Asselin filter, Ocean Model., 41, 53–66, doi:10.1016/j.ocemod.2011.11.002, 2012.

Mathews, T. and Fisher, N. S.: Trophic transfer of seven trace metals in a four-step marine food chain, Mar. Ecol.-Prog. Ser., 367, 23–33, doi:10.3354/meps07536, 2008.

MEXT: Report on the monitoring of radionuclides in fishery products, March 2011 to March 2014, Fisheries Agency of Japan, available at: http://www.mofa.go.jp/files/000040303.pdf (last access: 24 June 2015), 2014.

Monte, L., Perianez, R., Boyer, P., Smith, J. T., and Brittain, J. E.: The role of physical processes controlling the behaviour of radionuclide contaminants in the aquatic environment: a review of state-of-the-art modelling approaches, J. Environ. Radioactiv., 100, 779–784, doi:10.1016/j.jenvrad.2008.05.006, 2009.

Petrenko, A., Dufau, C., and Estournel, C.: Barotropic eastward currents in the western Gulf of Lion, north-western Mediterranean Sea, during stratified conditions, J. Marine Syst., 74, 406–428, doi:10.1016/j.jmarsys.2008.03.004, 2008.

BGD
12, 9497–9541, 2015

Povinec, P. P., Hirose, K., and Aoyama, M.: 6 – Pre-Fukushima Radioactivity of the Environment, in: Fukushima Accident, edited by: Aoyama, P. P. P. H., 277–323, Elsevier, Boston, available at: http://www.sciencedirect.com/science/article/pii/B9780124081321000061 (last access: 08 May 2015), 2013.

Pröhl, G.: Dosimetric models and data for assessing radiation exposures to biota, available at" https://wiki.ceh.ac.uk/download/attachments/115802176/fasset_d3.pdf?version=1&modificationDate=1263905014000&api=v2 (last access: 24 June 2015), 2003.

Rowan, D. J.: Bioaccumulation factors and the steady state assumption for cesium isotopes in aquatic foodwebs near nuclear facilities, J. Environ. Radioactiv., 121, 2–11, doi:10.1016/j.jenvrad.2012.03.008, 2013.

Sandberg, J., Kumblad, L., and Kautsky, U.: Can ECOPATH with ECOSIM enhance models of radionuclide flows in food webs? – an example for ^{14}C in a coastal food web in the Baltic Sea, J. Environ. Radioactiv., 92, 96–111, doi:10.1016/j.jenvrad.2006.09.010, 2007.

Sazykina, T. G.: ECOMOD – An ecological approach to radioecological modelling, J. Environ. Radioactiv., 50, 207–220, 2000.

Sushchenya, L. M.: Food rations, metabolism and growth of crustaceans, in: Marine food chains, edited by: Steele, J. H., 127–141„ 1970.

Thomann, R.: Equilibrium-Model of Fate of Microcontaminants in Diverse Aquatic Food-Chains, Can. J. Fish. Aquat. Sci., 38, 280–296, 1981.

Ulses, C., Estournel, C., de Madron, X. D., and Palanques, A.: Suspended sediment transport in the Gulf of Lions (NW Mediterranean): Impact of extreme storms and floods, Cont. Shelf Res., 28, 2048–2070, doi:10.1016/j.csr.2008.01.015, 2008.

UNCEAR: Report to the General Assembly, Scientific Annex a: Levels and Effects of Radiation Exposure due to the Nuclear Accident after the 2011 Great East-Japan Earthquake and Tsunami, in Sources, Effects and Risk of Ionizing Radiation, vol. 1, New York, 2014.

Vives i Batlle, J.: Dynamic modelling of radionuclide uptake by marine biota: application to the Fukushima nuclear power plant accident, J. Environ. Radioactiv., in press, doi:10.1016/j.jenvrad.2015.02.023, 2015.

Vives i Batlle, J., Wilson, R. C., and McDonald, P.: Allometric methodology for the calculation of biokinetic parameters for marine biota., Sci. Total Environ., 388, 256–69, doi:10.1016/j.scitotenv.2007.07.048, 2007.

Williams, L. G.: Uptake of Cesium137 by Cells and Detritus of Euglena and Chlorella, Limnol. Oceanogr., 5, 301–311, doi:10.4319/lo.1960.5.3.0201, 1960.

Yousef, Y. A., Padden, T. J., and Gloyna, E. F.: Diurnal changes in radionuclides uptake by phytoplankton in small scale ecosystems, available at: http://inis.iaea.org/Search/search.aspx?orig_q=RN:6180719 (last access: 19 February 2015), 1975.
Zhao, X. G., Wang, W. X., Yu, K. N., and Lam, P. K. S.: Biomagnification of radiocesium in a marine piscivorous fish, Mar. Ecol.-Prog. Ser., 222, 227–237, doi:10.3354/meps222227, 2001.

BGD
12, 9497–9541, 2015

Modelling of Fukushima-derived ^{137}Cs transfer to plankton populations

M. Belharet et al.

Table 1. Radioecological parameters obtained from the model calibration.

	Parameter	Unit	Value
μ_{ps}	Accumulation rate from water for PS	$L\,g^{-1}\,d^{-1}$	0.015
μ_{pl}	Accumulation rate from water for PL	$L\,g^{-1}\,d^{-1}$	0.015
μ_{zs}	Accumulation rate from water for ZS	$L\,g^{-1}\,d^{-1}$	5×10^{-4}
μ_{zl}	Accumulation rate from water for ZL	$L\,g^{-1}\,d^{-1}$	5×10^{-4}
μ_{zp}	Accumulation rate from water for ZP	$L\,g^{-1}\,d^{-1}$	10^{-3}
λ_{ps}	Small phytoplankton elimination rate	d^{-1}	0.5
λ_{pl}	Large phytoplankton elimination rate	d^{-1}	0.5
λ_{zs}	Small zooplankton elimination rate	d^{-1}	0.11
λ_{zl}	Large zooplankton elimination rate	d^{-1}	0.07
λ_{zp}	Predatory zooplankton elimination rate	d^{-1}	0.03
AE_z	^{137}Cs assimilation efficiency by zooplankton	No dim	0.75

BGD
12, 9497–9541, 2015

Table 2. Correlation coefficients (r) between the ingestion rates and the TTF of different zooplankton groups.

Parameter	TTF	Non-accidental		Accidental	
		Whole area	0–30 km	Whole area	0–30 km
IR_{ZS}	ZS	0.94	0.91	0.88	0.68
IR_{ZL}	ZL	0.85	0.84	0.77	0.46
IR_{ZP}	ZP	0.83	0.79	0.76	0.37

BGD
12, 9497–9541, 2015

Table 3. Parameter values used in the absorbed dose calculation. All units are in µGy h^{-1} per Bq kg^{-1}.

Parameter	Definition	Phytoplankton	Zooplankton
$DCC_{Cs\text{-}pk}$	Dose conversion coefficient for internal exposure	4.7×10^{-6}	4.6×10^{-4}
$DCC_{Cs\text{-}w\text{-}pk}$	Dose conversion coefficient for external exposure	1.1×10^{-4}	3.6×10^{-4}

BGD
12, 9497–9541, 2015

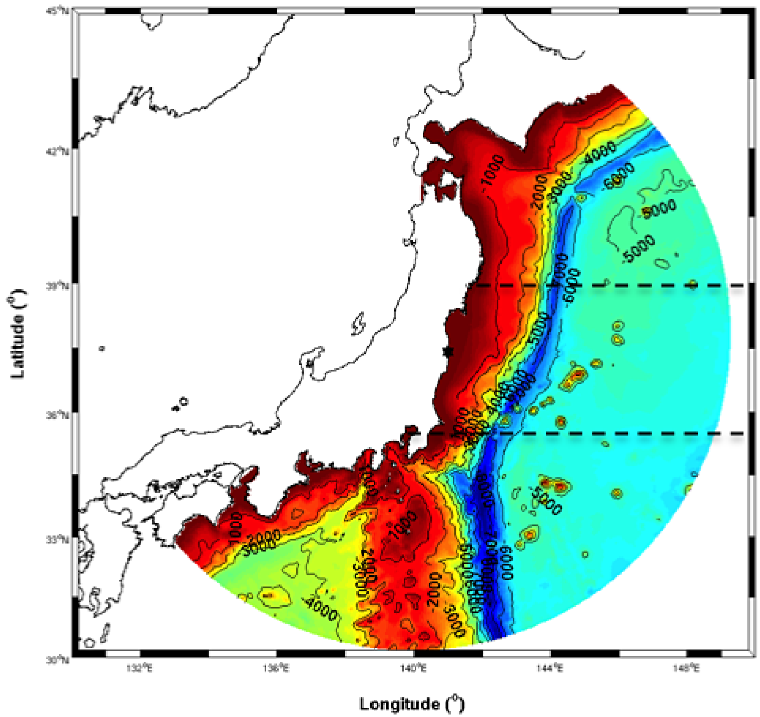

Figure 1. Numerical domain and its bathymetry. The dashed lines indicate the limits of the three regional areas: the subtropical region (latitude < 35° N), the transition region (35° N < latitude < 39° N), and the subarctic region (latitude > 39° N).

BGD
12, 9497–9541, 2015

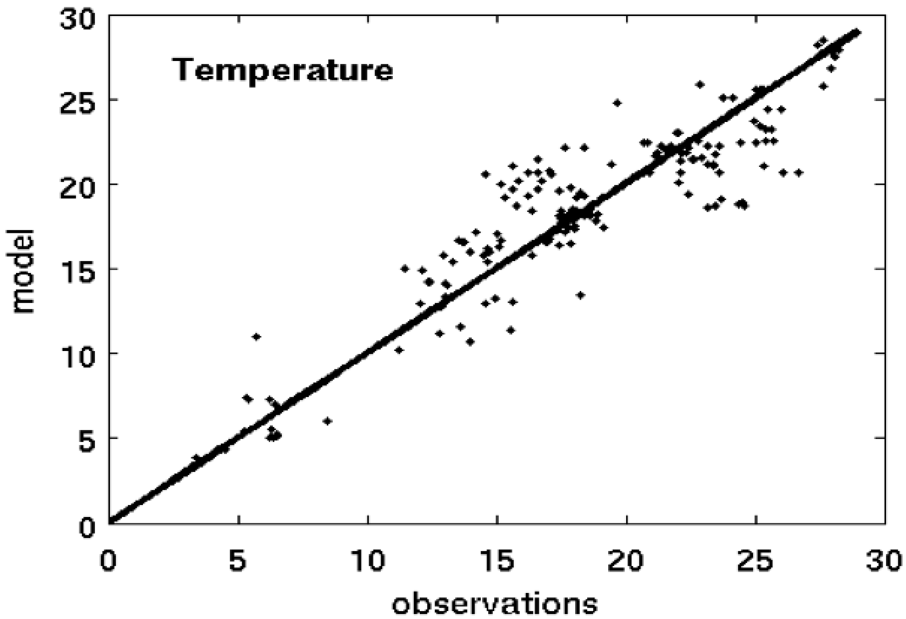

Figure 2. Comparison between the SYMPHONIE model temperature outputs and the field data observed in the whole study area.

BGD
12, 9497–9541, 2015

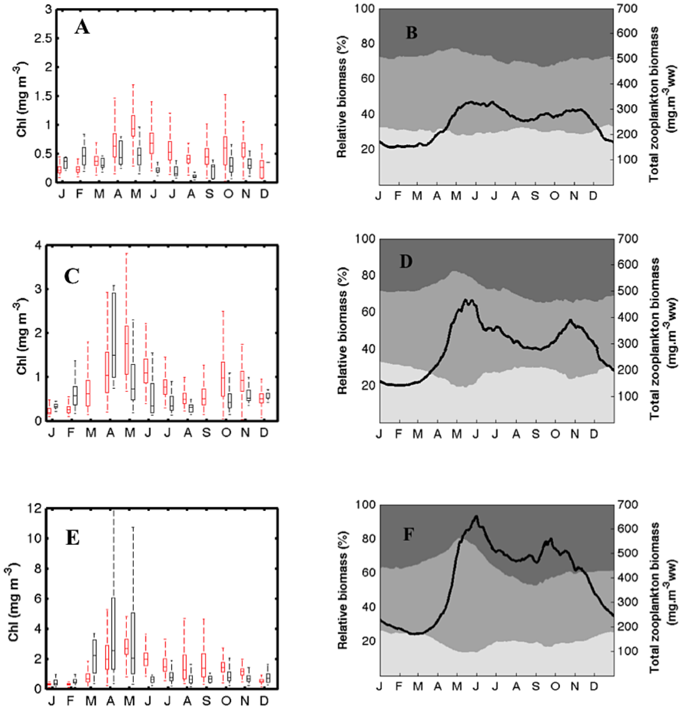

Figure 3. Left **(a, c, e)**: climatological seasonal cycle of integrated chlorophyll from in situ data (in black) and model results (in red) aggregated as monthly medians. In situ climatology data is derived from the Japan Oceanographic Data Center (JODC) dataset for the period (1990–2010). Model outputs are monthly medians for the period 2011–2012 and represented for the three regional areas described in Fig. 1. Right **(b, d, f)**: results of the two-year simulation of the total zooplankton biomass represented as the spatial median (dark line) and its taxonomic composition in the three regional areas described above: subtropical region **(a, b)**, transition region **(c, d)**, subarctic region **(e, f)**.

BGD
12, 9497–9541, 2015

Modelling of Fukushima-derived ^{137}Cs transfer to plankton populations

M. Belharet et al.

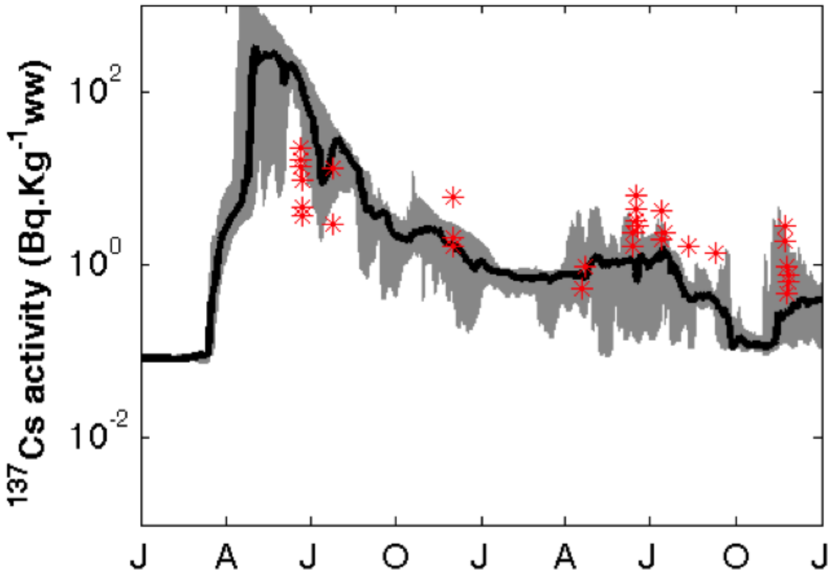

Figure 4. Results of the model calibration represented as the spatial median of the ^{137}Cs concentration mean in the three zooplankton groups situated in the Sendai Bay (35.6–36° N and 141–142° W). The red stars represent the field data of ^{137}Cs activity in zooplankton in the same location.

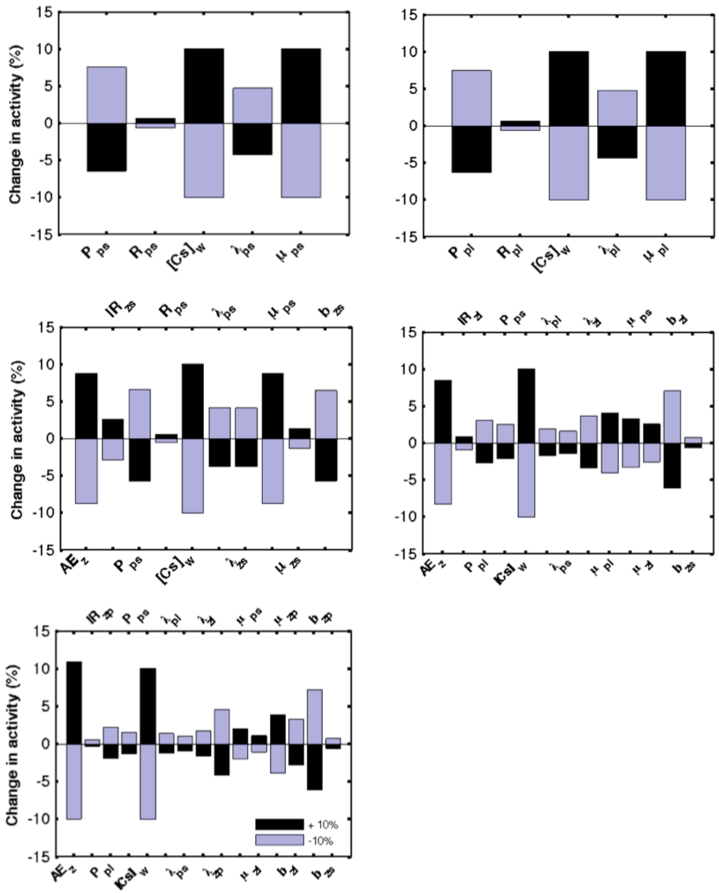

Figure 5. Sensitivity of activity estimates to a 10% change in the parameters of Eqs. (3) and (7) for all plankton groups considered in this study.

BGD
12, 9497–9541, 2015

Modelling of Fukushima-derived ^{137}Cs transfer to plankton populations

M. Belharet et al.

Title Page
Abstract | Introduction
Conclusions | References
Tables | Figures
◀| |▶
◀ ▶
Back | Close
Full Screen / Esc
Printer-friendly Version
Interactive Discussion

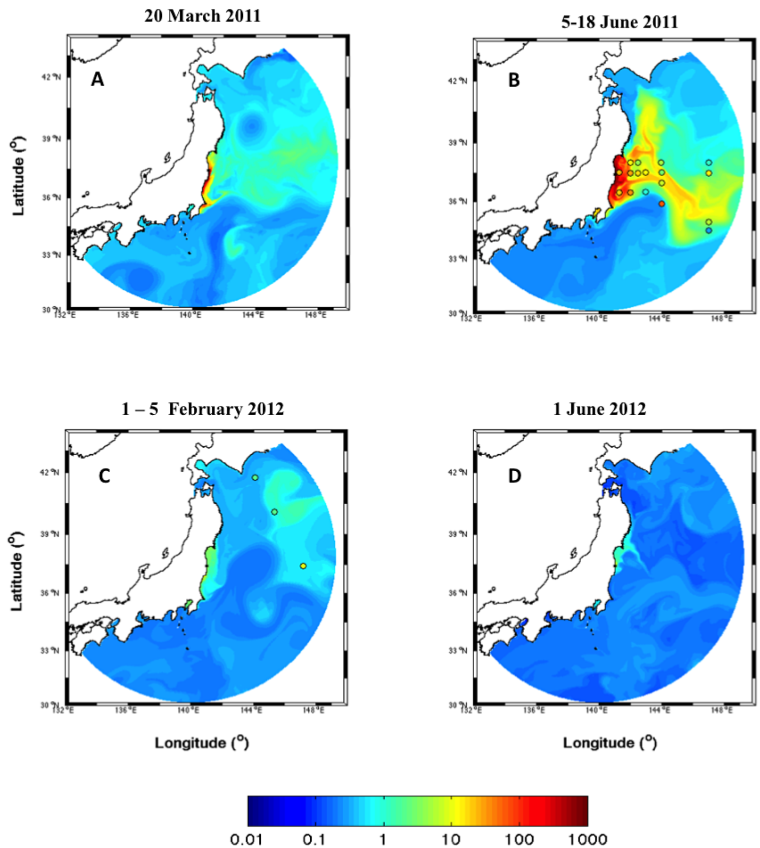

Figure 6. Spatial and temporal dynamics of the simulated ^{137}Cs activity concentration based on the dry weight in the large zooplankton. The coloured rounds in **(a)** and **(b)** represent the field data reported by Buesseler et al. (2012) and Kitamura et al. (2013), respectively.

BGD
12, 9497–9541, 2015

Title Page
Abstract | Introduction
Conclusions | References
Tables | Figures
◂| |▸
◂ ▸
Back | Close
Full Screen / Esc
Printer-friendly Version
Interactive Discussion

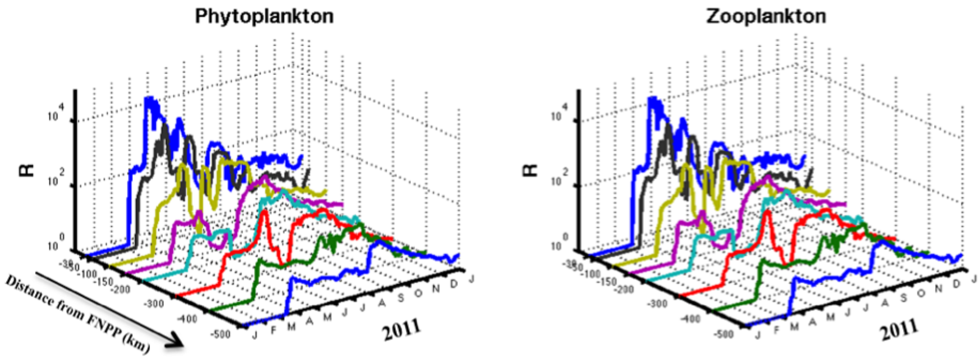

Figure 7. Calculated ratios (R) of ^{137}Cs concentration in phytoplankton and zooplankton in the accident situation to its concentration in the same population in the no-accident situation. The ratio was calculated for different sectors at various distances from FNPP.

BGD

12, 9497–9541, 2015

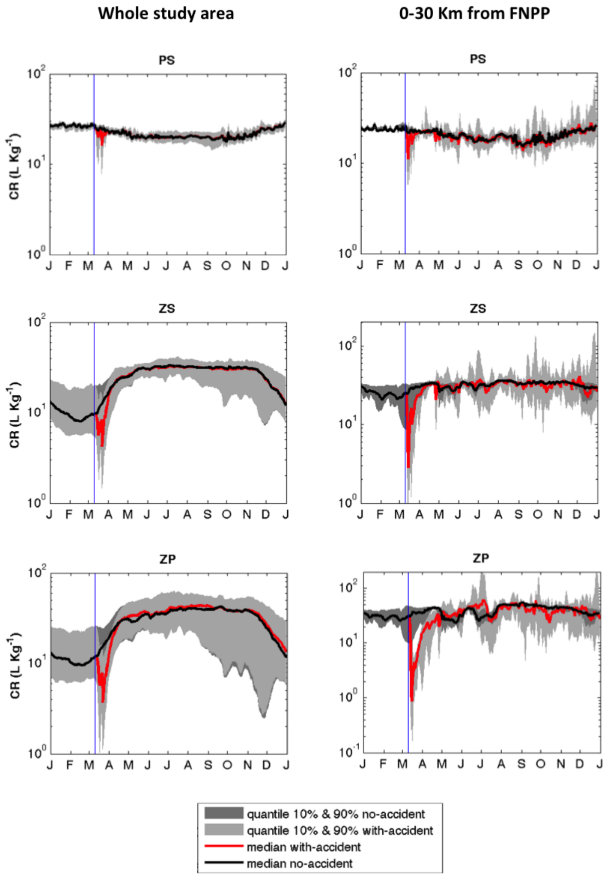

Figure 8. Results of concentration ratio estimated for small phytoplankton, large zooplankton and predatory zooplankton in the whole study area (left) and for those populations located at less than 30 km from FNPP (right). The blue vertical line separates the pre- and post-accident periods.

BGD
12, 9497–9541, 2015

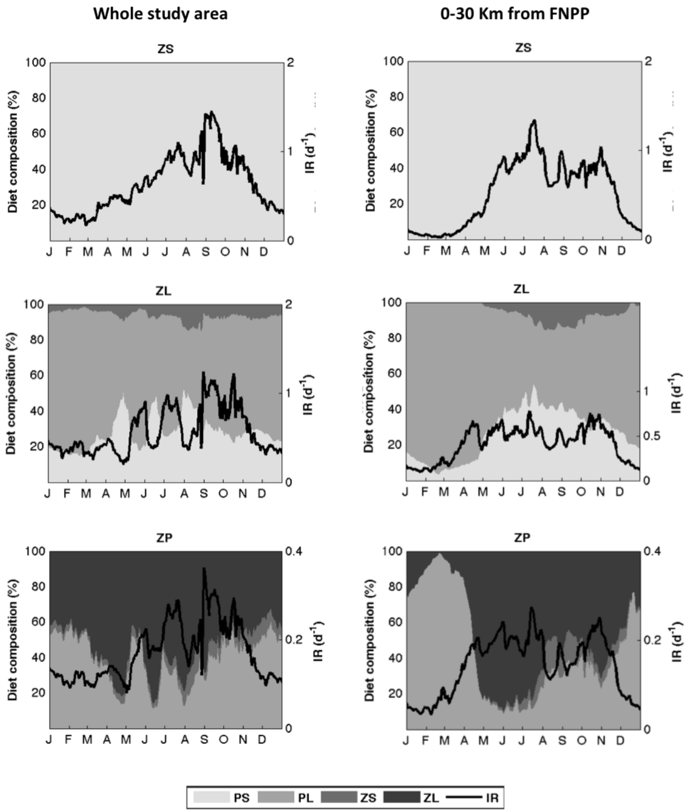

Figure 9. Food ingestion rate associated with the diet composition for the three groups of zooplankton in the areas located between 0–30 km (left) and for the zooplankton of the whole study area (right).

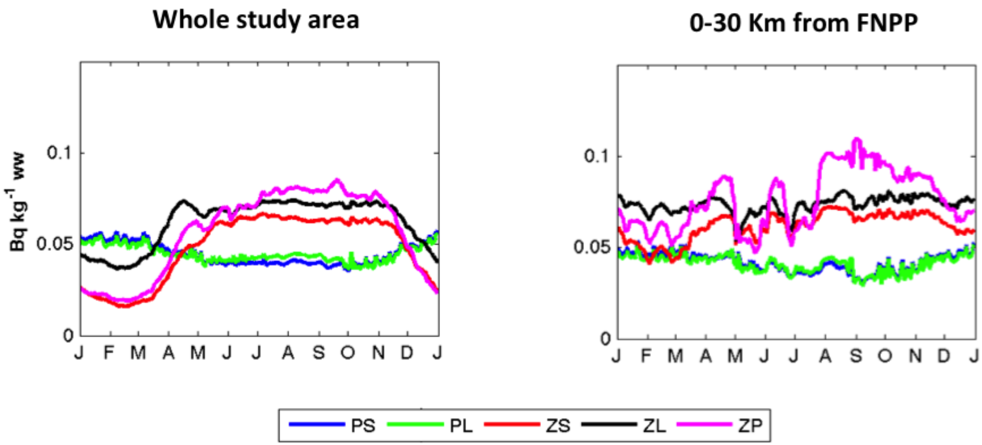

Figure 10. Dynamics of ^{137}Cs concentration in all plankton groups in the no-accident situation.

BGD
12, 9497–9541, 2015

Modelling of Fukushima-derived ^{137}Cs transfer to plankton populations

M. Belharet et al.

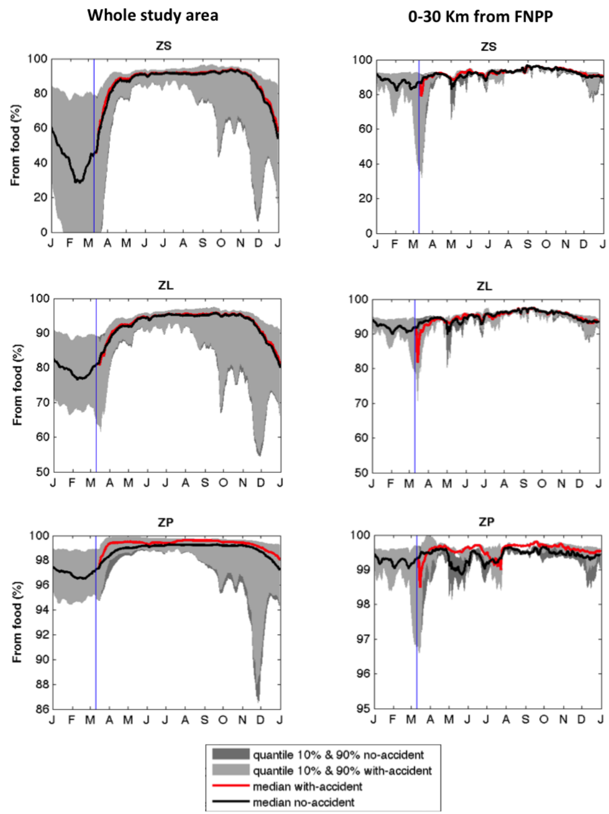

Figure 11. Relative fraction of ^{137}Cs accumulated from diet for the three functional groups of zooplankton calculated as the spatial median and quantiles of the whole study area (left) and in the sector located at less than 30 km from FNPP (right). The vertical blue line separates the pre- and post-accident periods.

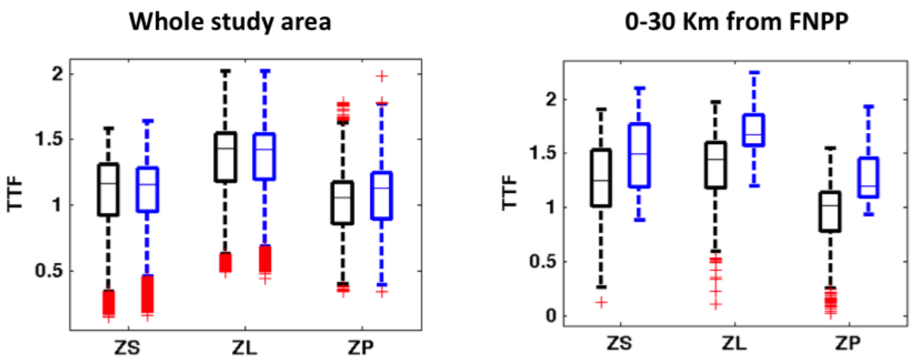

Figure 12. Boxplots of the Trophic Transfer Factor (TTF) calculated over 2011 for the three groups of zooplankton and for the two different spatial scales. The dark colour represents the accident situation and the blue colour represents the no-accident situation.

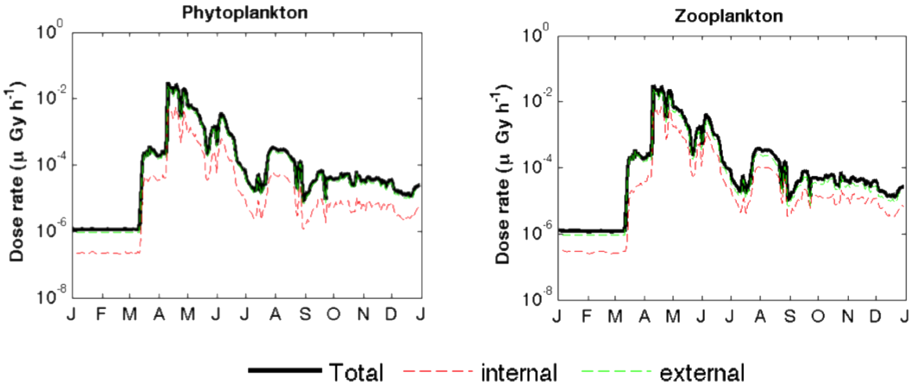

Figure 13. ^{137}Cs dose rates received by plankton populations located at less than 30 km from FNPP.